Supplementary Information

Mandy B. Freund[1,2,3,4,5], Gerhard Helle[4], Daniel F. Balting[4,6], Natasha Ballis[3,7], Gerhard H. Schleser[8], and Ulrich Cubasch[5]

[1] *CSIRO Oceans and Atmosphere, Melbourne, VIC, Australia*

[2] *School of Geography, Earth and Atmospheric Sciences, University of Melbourne, Parkville, VIC 3010, Australia*

[3] *Climate and Energy College, University of Melbourne, Parkville, VIC 3010, Australia*

[4] *German Research Centre for Geosciences, Climate Dynamics and Landscape Evolution, Potsdam 14473, Germany*

[5] *Freie Universität Berlin, Department of Earth Science,Institute for Meteorology, 12165 Berlin, Germany*

[6] *Alfred-Wegener-Institute, Bremerhaven, 27570, Germany*

[7] *Environmental Hydrology and Water Resources, Department of Infrastructure Engineering, University of Melbourne, Parkville, VIC, 3010 Australia*

[8] *Institute of Bio- and Geosciences IBG-3, Forschungszentrum Julich, Julich 52428, Germany*

Supplementary Table 1. Details of tree ring isotope sites

Code	Site name	Genus	Species	Altitude	Lat	Lon	First Year	Last Year	Reference
Vich	Mount Vichren	*Pinus*	*heldreichii*	1900	41.46	23.24	1800	2005	1–6
Poll	Monte Pollino	*Pinus*	*leucodermis*	1900	39.58	16.16	1604	2003	1–6
Caz	Cazorla	*Pinus*	*nigra*	1820	37.53	-2.57	1600	2002	1;2;4–14
Peda	Pedraforca	*Pinus*	*uncinata*	2120	42.13	1.42	1600	2003	1;2;4–14
Pina	Pinar de Lillo	*Pinus*	*sylvestris*	1600	42.57	-5.34	1600	2002	1;2;4–14
Isib	Isibeli	*Juniper*	*excelsa*	1800	37.06	30.45	1850	2005	1;2;4–6;15
Col	Col Du Zad	*Cedrus*	*atlantica*	2200	32.59	-5.14	1600	2000	1–6
Vinu	Vinuesa	*Pinus*	*uncinata*	999	42.00	2.45	1850	2002	1;2;7;8;16
Cave	Cavergno	*Quercus*	*petraea*	900	46.21	8.36	1637	2002	1;2;4–6;17–19
Dles	Dleskovska	*Larix*	*decidua*	1700	46.30	14.30	1600	2005	20–22
Renn	Renn	*Quercus*	*robur*	100	48.25	-1.70	1751	1998	23–28
Poel	Poellau	*Pinus*	*nigra*	500	47.95	16.06	1600	2002	1;2;4–6
Laiz	Laizer	*Quercus*	*petraea*	300	48.18	16.20	1600	2003	1;2;4–6;29;30
Inar	Inari	*Pinus*	*sylvestris*	150	68.93	28.42	1600	2002	1;2;4–6
Siva	Sivakkovaara	*Pinus*	*sylvestris*	200	62.98	30.98	1600	2002	1;2;4–6
Dran	Dransfeld	*Quercus*	*petraea*	320	51.50	9.78	1776	2002	1;2;4–6
Pane	Panemunes	*Pinus*	*sylvestris*	45	54.88	23.97	1816	2002	1–6
NiepQ	Niepolomice	*Quercus*	*robur*	190	50.12	20.38	1627	2003	1;2;4–6;31–38
Suwa	Suwalki	*Pinus*	*sylvestris*	160	54.10	22.93	1600	2004	1;2;4–6
NiepP	Niepolomice	*Pinus*	*sylvestris*	190	50.12	20.38	1627	2003	1;2;4–6
Vig	Vigera	*Pinus*	*sylvestris*	1400	46.50	8.77	1675	2003	1;2;4–6;17;19
Gutu	Gutuli	*Pinus*	*sylvestirs*	800	62.00	12.18	1600	2003	1;2;4–6
Font	Fontainebleau	*Quercus*	*petraea*	100	48.38	2.67	1600	2000	1;2;4–6;23–28
Wobu	Woburn	*Pinus*	*sylvestris*	10	51.98	-0.59	1604	2003	1;2;4–6;39–42
Plie	Plieningen	*Quercus*	*petraea*	340	48.42	9.13	1822	1999	1;2;4–6
Loch	Lochwood	*Quercus*	*petraea*	175	55.27	-3.43	1749	2003	1;2;4–6;40

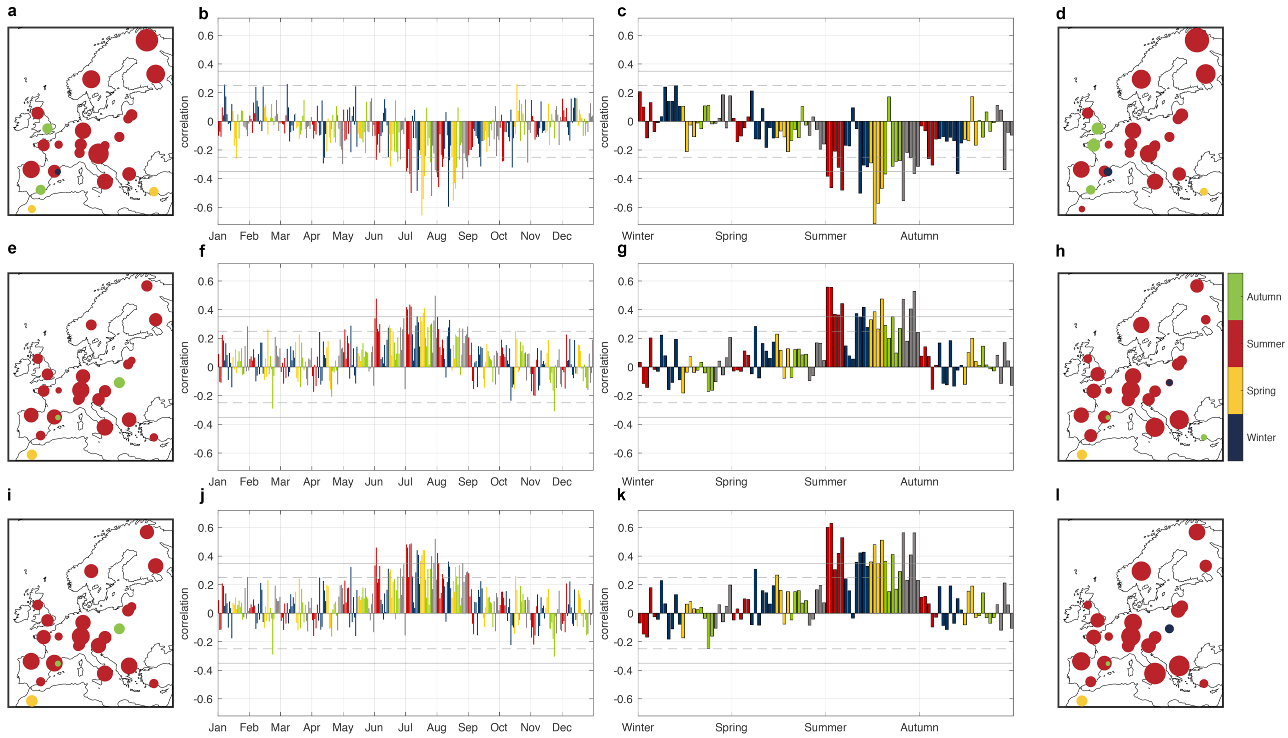

Supplementary Figure 1. Correlations of $\delta^{13}C$ records and regional climate variables a,b,e,f,i,j Monthly correlations with climate variables temperature **(a,b)**, precipitation **(e,f)** and SPEI-01 **(i,j)** as spatial maps of the leading season **(a,e,i)** and individually for each month **(b,f,j)**. **c,d,g,h,k,l** Seasonal correlations with climate variables temperature **(c,d)**, precipitation **(g,h)** and SPEI-01 **(k,l)** as spatial maps of the leading season **(d,h,l)** and individually for each month **(c,g,k)**. Records are color coded in descending order in red (Vich, Poll, Caz, Peda, Pina), in blue (Isib, Col, Vinu, Cave, Dles, Renn, Poel), in yellow (Laiz, Inar, Siva, Dran) in green (Pane, NiepQ, Suwa, NiepP, Vig) and in grey (Gutu, Font, Wobu, Plie, Loch). All correlations are calculated for the common period of 1901-1998. For the spatial maps **(a,e,i,d,h,l)**, the leading season is assigned to the highest seasonal/monthly correlation to the closest gridbox within 60 km.

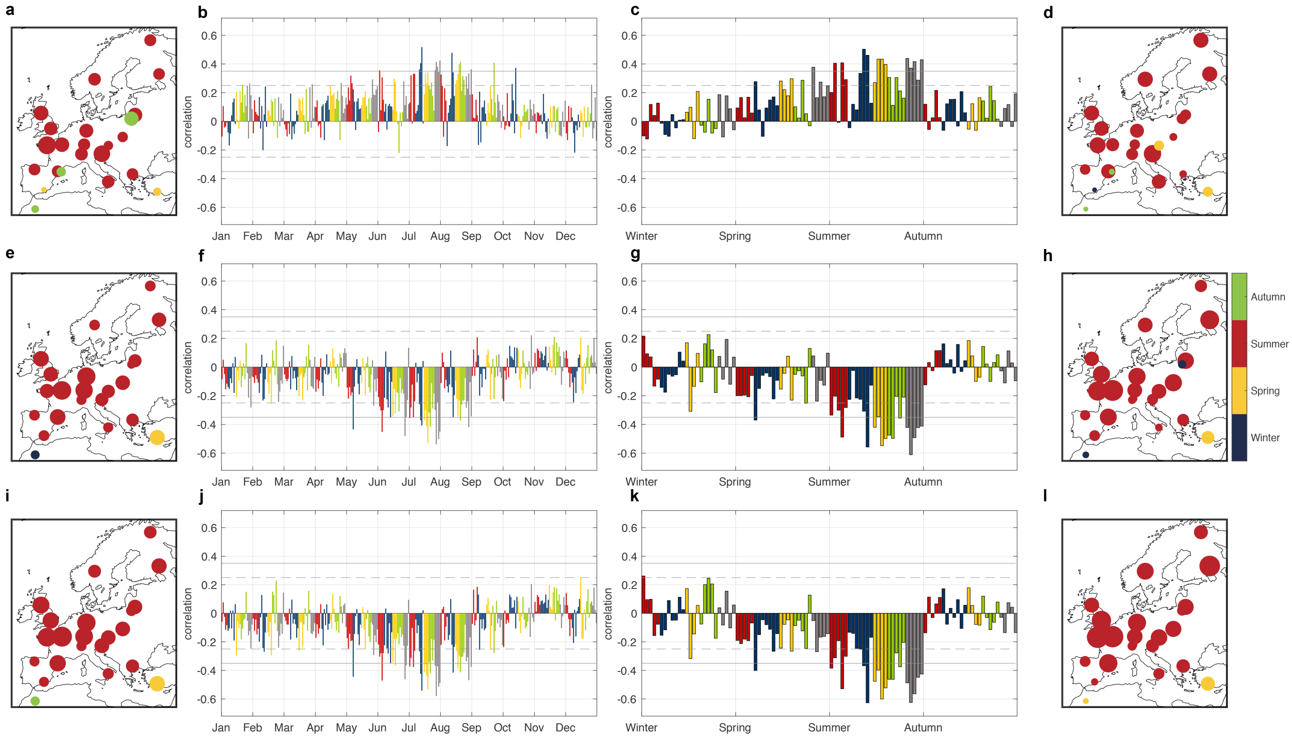

Supplementary Figure 2. Correlations of $\delta^{18}O$ records and regional climate variables a,b,e,f,i,j Monthly correlations with climate variables temperature **(a,b)**,precipitation **(e,f)** and SPEI-01 **(i,j)** as spatial maps of the leading season **(a,e,i)** and individually for each month **(b,f,j)**. **c,d,g,h,k,l** Seasonal correlations with climate variables temperature **(c,d)**, precipitation **(g,h)** and SPEI-01 **(k,l)** as spatial maps of the leading season **(d,h,l)** and individually for each month **(c,g,k)**. Records are color coded in descending order in red (Vich, Poll, Caz, Peda, Pina), in blue (Isib, Col, Vinu, Cave, Dles, Renn, Poel), in yellow (Laiz, Inar, Siva, Dran) in green (Pane, NiepQ, Suwa, NiepP, Vig) and in grey (Gutu, Font, Wobu, Plie, Loch). All correlations are calculated for the common period of 1901-1998. For the spatial maps **(a,e,i,d,h,l)**, the leading season is assigned to the highest seasonal/monthly correlation to the closest gridbox within 60 km.

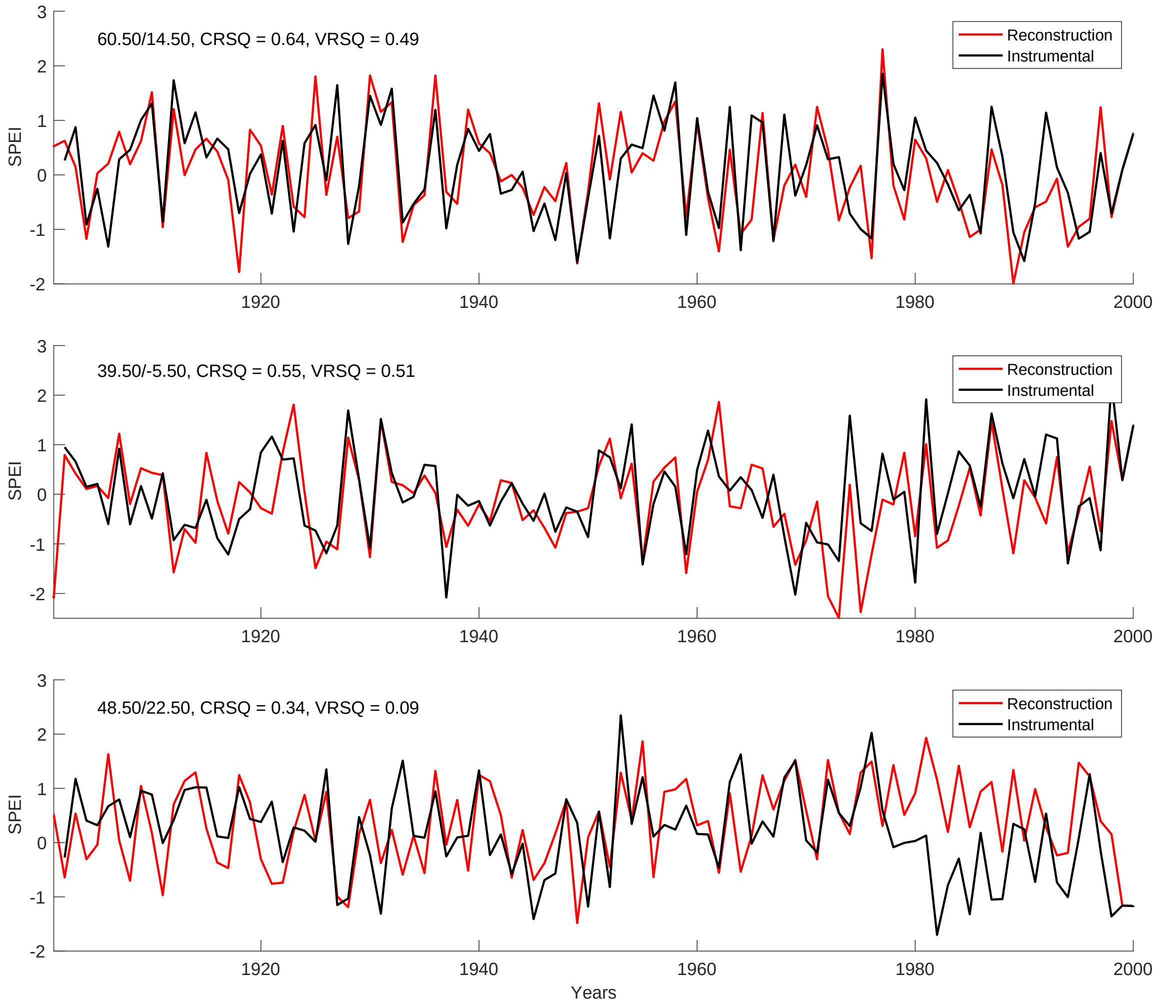

Supplementary Figure 3. Comparison of reconstructed and instrumental SPEI-02 (JA) for selected gridpoints Location of individual gridpoints given by insets latitude and longitude, and calibration CRSQ and verification VRSQ.

Supplementary Table 2. Correlation of the SPEI reconstruction and long instrumental records Closest gridpoint correlation of the SPEI reconstruction and long instrumental precipitation and temperature records prior to the calibration period 1912. Only significant correlations are shown at the 95th confidence level.
.

Station Name	Lat	Lon	Start Temp	Start Precip	Corr(Temp) Europe	Corr(Temp) Local	Corr(Precip) Local
Budapest	47.50	19.00	1780	1841	-0.42	-0.51	0.34
Dahlem	52.60	13.40	1851	1848	-0.45	-0.55	0.35
Debilt	45.40	12.00	1706	1725	-0.32	-0.36	0.39
Greenwich	51.50	0.00	1851	1820	-0.33	-0.60	0.52
Kopenhagen	55.68	12.53	1851	1890	-0.32	-0.56	0.52
Lisbon	38.70	-9.10	1855	1864		-0.32	
Marsailie	43.30	5.40	1851	1810	-0.32	-0.51	0.11
Milan	45.50	9.30	1862	1764		-0.54	0.31
Munich	48.10	11.70	1781	1848	-0.46	-0.54	0.60
Oslo	59.95	10.72	1851	1895	-0.25	-0.57	0.26
Oxford	51.70	-1.20	1851	1767	-0.31	-0.55	0.47
Paris	48.80	2.50	1851	1770	-0.32	-0.61	0.43
Prague	50.10	14.30	1851	1805	-0.47	-0.49	0.29
Riga	56.97	24.07	1851	1891		-0.61	0.47
Rom	41.80	12.20	1851	1871	-0.28	-0.26	0.48
Stuttgart	48.80	9.20	1856	1825	-0.44	-0.61	0.25
Uccle	50.80	4.40	1851	1833	-0.39	-0.52	0.52
Warsaw	52.10	21.00	1851	1885	-0.47	-0.62	0.66

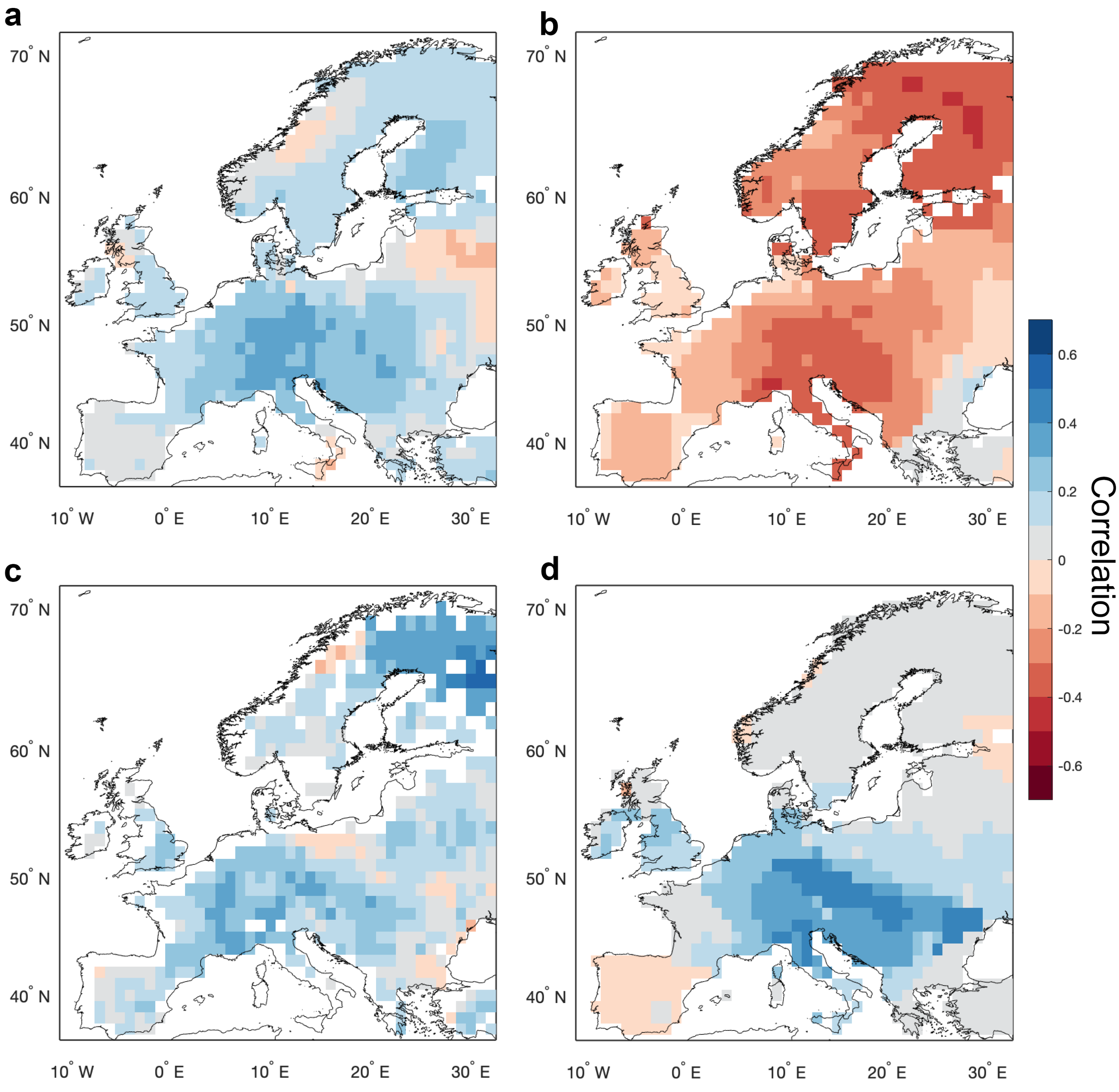

Supplementary Figure 4. Correlations with published reconstructions Point-wise correlation of the SPEI summer reconstruction with **(a)** a spatial precipitation reconstruction[43], **(b)** spatial temperature reconstruction[44],**(c)** spatial PDSI reconstruction[45] and **(d)** PDSI tree-ring isotope reconstruction for central Europe[46] prior to 1900.

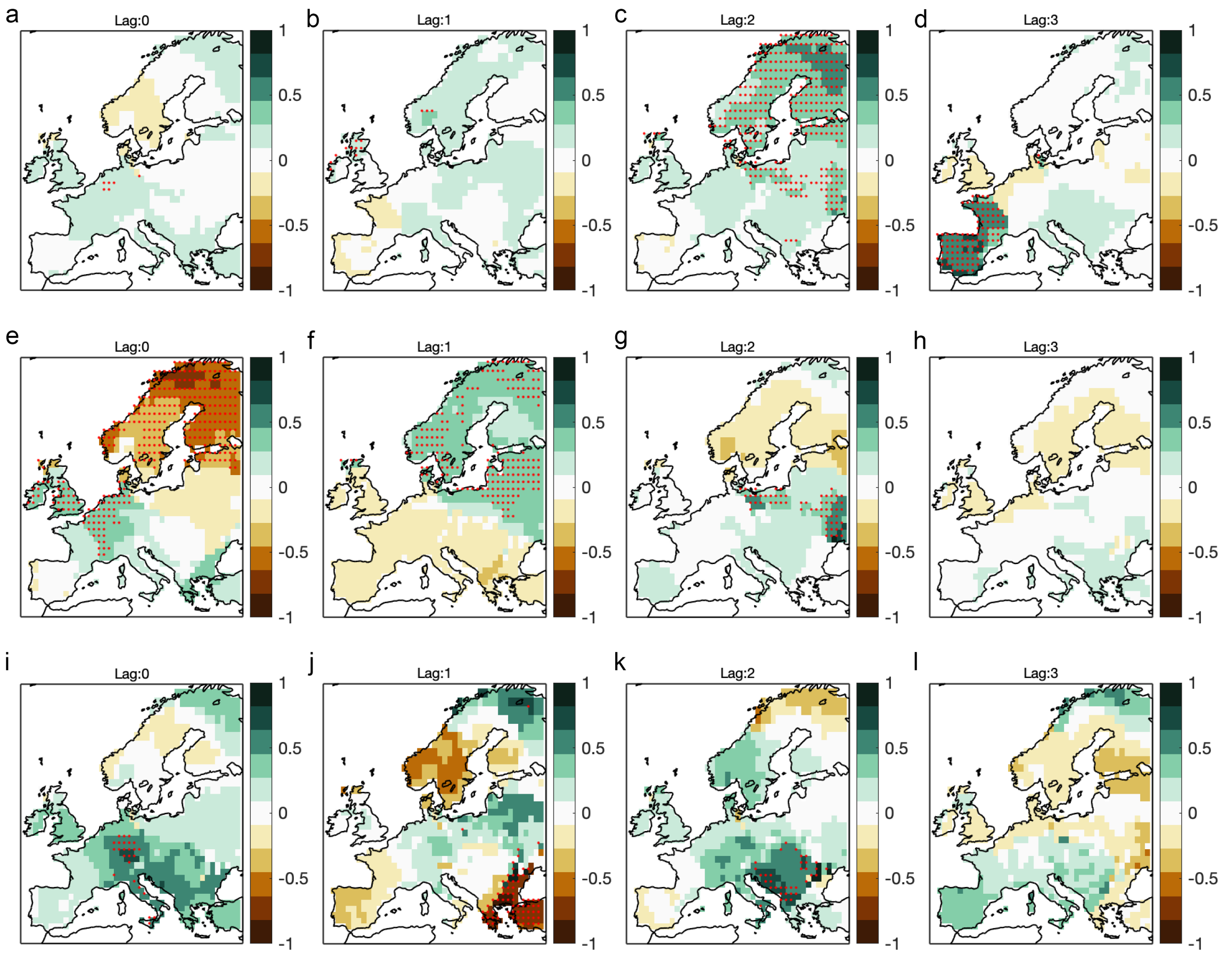

Supplementary Figure 5. Impact of volcanic eruptions Composites of reconstructed SPEI during different volcanic eruption datasets. Shown are the composite means with stipplings indicating significance at the 95% confidence level based on bootstrapped sampling. **(a-d)** SEA1 according to[47]. **(e-h)** Northern Hemisphere eruption years[48]. **(i-l)** TVEP eruptions years[49].

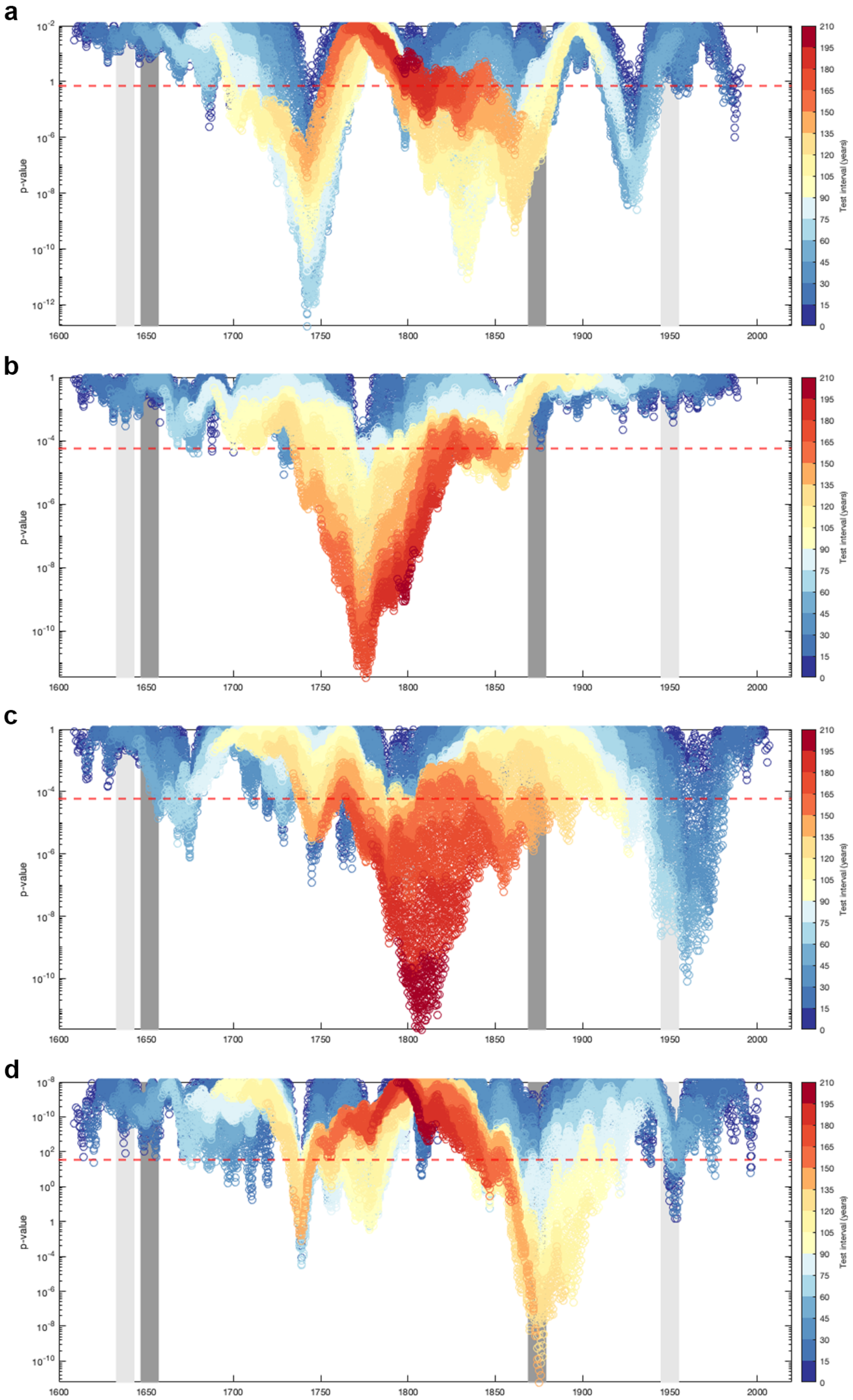

Supplementary Figure 6. Comparison of change points Change points of different European reconstructions of **(a)** average temperature[44], **(b)** average precipitation[43] ,**(c)** scPDSI for central Europe[46] and **(d)** average scPDSI reconstruction[45]. Vertical lines indicate significant long-term (dark, >30 years) and short-term (light) change points identified in our study.

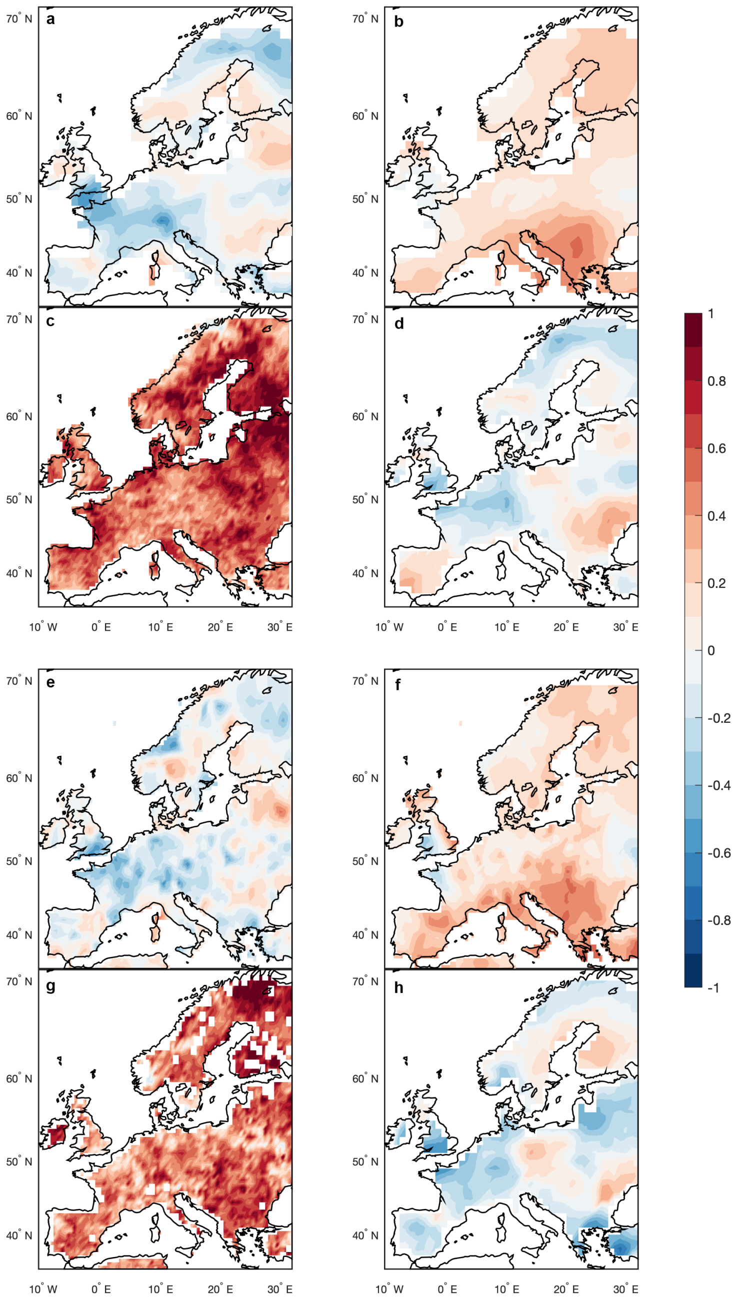

Supplementary Figure 7. Comparison of low- to high-frequency variability Representation of high- to low frequency spectra of observed **(a)** and reconstructed **(e)** precipitation[43], observed **(b)** and reconstructed **(f)** temperature[44], observed **(c)** and reconstructed **(g)** summer scPDSI[45] and observed **(d)** and reconstructed **(h)** SPEI (this study). Values indicate the *beta* value according to[?] .

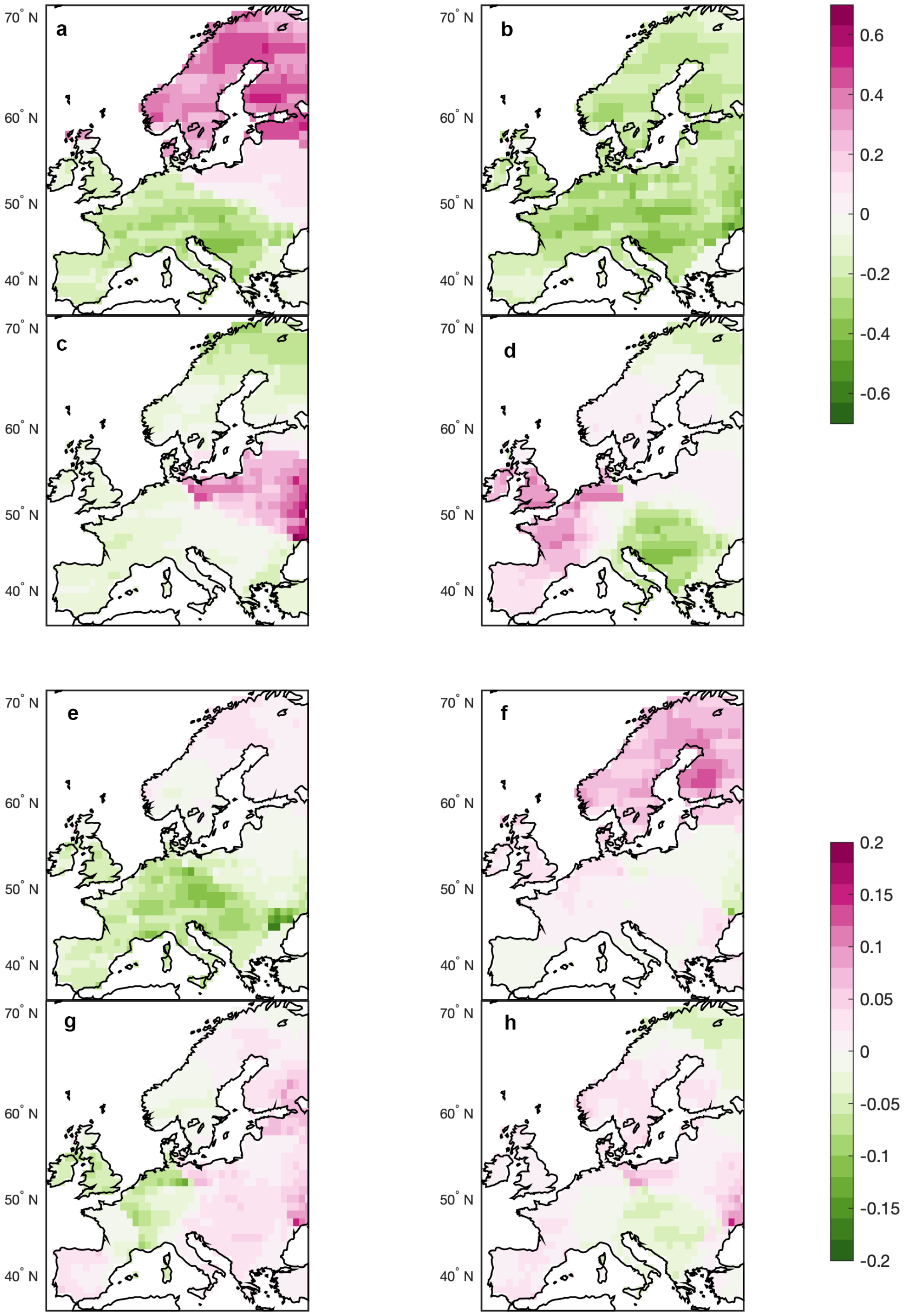

Supplementary Figure 8. Principle Components Principle Components (PC) at annual time scale explain 24.5% (PC1 **a,**) , 20.7% (PC2 **b,**), 10.7 % (PC3 **c,**) and 10% (PC4 **d,**) of the overall variance. Principle Components (PC) at decadal time scale explain 24.6% (PC1 **e,**) , 20.7% (PC2 **f,**), 13.7 % (PC3 **g,**) and 8.3% (PC4 **h,**) of the overall variance.

Supplementary References

[1] Shestakova, T. A. *et al.* Spatio-temporal patterns of tree growth as related to carbon isotope fractionation in European forests under changing climate. *Glob. Ecol. Biogeogr.* **28**, 1295–1309 (2019).

[2] Balting, D. F. *et al.* Large-scale climate signals of a European oxygen isotope network from tree rings. *Clim. Past* **17**, 1005–1023 (2021).

[3] Keller, K. M. *et al.* 20th century changes in carbon isotopes and water-use efficiency: tree-ring-based evaluation of the CLM4.5 and LPX-Bern models. *Biogeosciences* **14**, 2641–2673 (2017).

[4] Treydte, K. *et al.* Signal strength and climate calibration of a European tree-ring isotope network. *Geophys. Res. Lett.* **34**, 224 (2007).

[5] Frank, D. C. *et al.* Water-use efficiency and transpiration across European forests during the Anthropocene. *Nat. Clim. Chang.* **5**, 579–583 (2015).

[6] Saurer, M. *et al.* Spatial variability and temporal trends in water-use efficiency of European forests. *Glob. Chang. Biol.* **20**, 3700–3712 (2014).

[7] Andreu, L., Planells, O., Gutierrez, E., Helle, G. & Schleser, G. H. Climatic significance of tree-ring width and delta 13 C in a Spanish pine forest network. *Tellus B* **60**, 771–781 (2008).

[8] Andreu Hayles, L. *et al.* Long tree-ring chronologies reveal 20th century increases in water-use efficiency but no enhancement of tree growth at five Iberian pine forests. *Glob. Chang. Biol.* **17**, 2095–2112 (2011).

[9] Dorado Liñán, I. *et al.* Estimating 750 years of temperature variations and uncertainties in the Pyrenees by tree-ring reconstructions and climate simulations. *Clim. Past* **8**, 919–933 (2012).

[10] Liñán, I. D., Gutierrez, E., Andreu Hayles, L., Heinrich, I. & Helle, G. Potential to explain climate from tree rings in the south of the Iberian Peninsula. *Clim. Res.* **55**, 119–134 (2012).

[11] Dorado Liñán, I. *et al.* Age effects and climate response in trees: a multi-proxy tree-ring test in old-growth life stages. *Eur. J. For. Res.* **131**, 933–944 (2012).

[12] Liñán, I. D. *et al.* Pooled versus separate measurements of tree-ring stable isotopes. *Sci. Total. Environ. The* **409**, 2244–2251 (2011).

[13] Andreu Hayles, L. *et al.* 400 Years of summer hydroclimate from stable isotopes in Iberian trees. *Clim. Dyn.* **49**, 143–161 (2016).

[14] Dorado Liñán, I. *et al.* Changes in surface solar radiation in Northeastern Spain over the past six centuries recorded by tree-ring δ13C. *Clim. Dyn.* **47**, 937–950 (2015).

[15] Heinrich, I., Touchan, R., Dorado Liñán, I., Vos, H. & Helle, G. Winter-to-spring temperature dynamics in Turkey derived from tree rings since AD 1125. *Clim. Dyn.* (2013).

[16] Planells, O., Gutierrez, E., Helle, G. & Schleser, G. H. A forced response to twentieth century climate conditions of two Spanish forests inferred from widths and stable isotopes of tree rings. *Clim. change* **97**, 229–252 (2009).

[17] Kress, A. *et al.* A 350 year drought reconstruction from Alpine tree ring stable isotopes. *Glob. Biogeochem. Cycles* **24** (2010).

[18] Reynolds-Henne, C. E. *et al.* Temporal stability of climate-isotope relationships in tree rings of oak and pine (Ticino, Switzerland). *Glob. Biogeochem. Cycles* **21** (2007).

[19] Saurer, M. *et al.* Influence of atmospheric circulation patterns on the oxygen isotope ratio of tree rings in the Alpine region. *J. Geophys. Res. Atmospheres –2012)* **117** (2012).

[20] Hafner, P. *et al.* Climate signals in the ring widths and stable carbon, hydrogen and oxygen isotopic composition of Larix decidua growing at the forest limit in the southeastern European Alps. *Trees* **25**, 1141–1154 (2011).

[21] Hafner, P. *et al.* A 520 year record of summer sunshine for the eastern European Alps based on stable carbon isotopes in larch tree rings. *Clim. Dyn.* **43**, 971–980 (2014).

[22] Levanic, T., Jevšenak, J. & Hafner, P. Stable Isotopes Reveal Climate Signal Hidden in Tree Rings of Endemic Balkan Pines. *Atmosphere* **11**, 135 (2020).

[23] Etien, N. *et al.* Summer maximum temperature in northern France over the past century: instrumental data versus multiple proxies (tree-ring isotopes, grape harvest dates and forest fires). *Clim. change* **94**, 429–456 (2009).

[24] Daux, V. *et al.* Comparisons of the Performance of δ13C and δ18O of Fagus sylvatica, Pinus sylvestris, and Quercus petraea in the Record of Past Climate Variations. *J. Geophys. Res. Biogeosciences* **123**, 1145–1160 (2018).

[25] Labuhn, I. *et al.* French summer droughts since 1326 CE: a reconstruction based on tree ring cellulose ¡i¿δ¡/i¿¡sup¿18¡/sup¿O. *Clim. Past* **12**, 1101–1117 (2016).

[26] Labuhn, I. *et al.* Tree age, site and climate controls on tree ring cellulose δ18O: A case study on oak trees from south-western France. *Dendrochronologia* **32**, 78–89 (2014).

[27] Masson-Delmotte, V. *et al.* Changes in European precipitation seasonality and in drought frequencies revealed by a four-century-long tree-ring isotopic record from Brittany, western France. *Clim. Dyn.* **24**, 57–69 (2005).

[28] Raffalli-Delerce, G. *et al.* Reconstruction of summer droughts using tree-ring cellulose isotopes: a calibration study with living oaks from Brittany (western France). *Tellus B: Chem. Phys. Meteorol.* **56**, 160–174 (2004).

[29] Weigl, M., Grabner, M., Helle, G., Schleser, G. H. & Wimmer, R. Characteristics of radial growth and stable isotopes in a single oak tree to be used in climate studies. *Sci. Total. Environ. The* **393**, 154–161 (2008).

[30] Haupt, M., Weigl, M., Grabner, M. & Boettger, T. A 400-year reconstruction of July relative air humidity for the Vienna region (eastern Austria) based on carbon and oxygen stable isotope ratios in tree-ring latewood cellulose of oaks (Quercus petraea Matt. Liebl.). *Clim. change* **105**, 243–262 (2011).

[31] Sensuła, B. M. The Impact of Climate, Sulfur Dioxide, and Industrial Dust on δ18O and δ13C in Glucose from Pine Tree Rings Growing in an Industrialized Area in the Southern Part of Poland. *Water, air, soil pollution* **227**, 106–13 (2016).

[32] Sensuła, B. & Wilczyński, S. Tree-ring widths and the stable isotope composition of pine tree-rings as climate indicators in the most industrialised part of Poland during CO elevation. *Geochronometria* **45**, 130–145 (2018).

[33] Sensuła, B., Michczyński, A., Piotrowska, N. & Wilczyński, S. Anthropogenic CO2 Emission Records in Scots Pine Growing in the Most Industrialized Region of Poland from 1975 to 2014. *Radiocarb.* **60**, 1041–1053 (2018).

[34] Szczepanek, M. G. *et al.* Hydrogen, carbon and oxygen isotopes in pine and oak tree rings from southern Poland as climatic indicators in years 1900 - 2003. *Geochronometria* (2006).

[35] Pazdur, A. *et al.* Carbon Isotopes in Tree Rings: Climate and the Suess Effect Interferences in the Last 400 Years. *Radiocarb.* **49**, 775–788 (2007).

[36] Pazdur, A. *et al.* Carbon Isotope Composition of Atmospheric Carbon Dioxide in Southern Poland: Imprint of Anthropogenic CO2 Emissions in Regional Biosphere. *Radiocarb.* **55**, 848–864 (2013).

[37] Pawelczyk, S., Pazdur, A. & Halas, S. Stable carbon isotopic composition of tree rings from a pine tree from Augustów Wilderness, Poland, as a temperature and local environment conditions indicator. *Isot. environmental health studies* **40**, 145–154 (2004).

[38] Pawełczyk, S. & Pazdur, A. Carbon Isotopic Composition of Tree Rings as A Tool for Biomonitoring CO2 Level. *Radiocarb.* **46**, 701–719 (2004).

[39] Rinne, K. T., Loader, N. J., Switsur, V. R. & Waterhouse, J. S. 400-year May-August precipitation reconstruction for Southern England using oxygen isotopes in tree rings. *Quat. Sci. Rev.* **60**, 13–25 (2013).

[40] Young, G. H. F. *et al.* Oxygen stable isotope ratios from British oak tree-rings provide a strong and consistent record of past changes in summer rainfall. *Clim. Dyn.* 1–14 (2015).

[41] Young, G. *et al.* Central England temperature since AD 1850: the potential of stable carbon isotopes in British oak trees to reconstruct past summer temperatures. *J. Quat. Sci.* **27**, 606–614 (2012).

[42] Rinne, K. T., Loader, N. J., Switsur, V. R., Treydte, K. & Waterhouse, J. S. Investigating the influence of sulphur dioxide (SO2) on the stable isotope ratios (δ13C and δ18O) of tree rings. *Geochimica et Cosmochimica Acta* **74**, 2327–2339 (2010).

[43] Pauling, A., Luterbacher, J., Casty, C. & Wanner, H. Five hundred years of gridded high-resolution precipitation reconstructions over Europe and the connection to large-scale circulation. *Clim. Dyn.* **26**, 387–405 (2005).

[44] Luterbacher, J., Dietrich, D., Xoplaki, E., Grosjean, M. & Wanner, H. European seasonal and annual temperature variability, trends, and extremes since 1500. *Sci.* **303**, 1499–1503 (2004).

[45] Cook, E. R. *et al.* Old World megadroughts and pluvials during the Common Era. *Sci. Adv.* **1**, e1500561 (2015).

[46] Büntgen, U. *et al.* Recent European drought extremes beyond Common Era background variability. *Nat. Geosci.* 1–19 (2021).

[47] Esper, J. *et al.* European summer temperature response to annually dated volcanic eruptions over the past nine centuries. *Bull. volcanology* **75**, 1–14 (2013).

[48] Toohey, M. & Sigl, M. Volcanic stratospheric sulfur injections and aerosol optical depth from 500 BCE to 1900 CE. *Earth Syst. Sci. Data* 809–831 (2017).

[49] Tejedor, E., Steiger, N. J., Smerdon, J. E., Serrano-Notivoli, R. & Vuille, M. Global hydroclimatic response to tropical volcanic eruptions over the last millennium. *Proc. Natl. Acad. Sci.* **118** (2021).